Analysis of Fault Location Algorithms with Electromagnetic Transients Program

Carlos Eduardo de Morais Pereira
Department of Electrical Engineering and Automation
Escola Politécnica da Universidade de São Paulo
São Paulo, Brasil

Luiz Cera Zanetta Jr
Department of Electrical Engineering and Automation
Escola Politécnica da Universidade de São Paulo
São Paulo, Brasil

Abstract - **In this work, a comparative study of some fault location algorithms in transmission lines is presented, using electromagnetic transients program. Calculation of the fault-distance was carried out by using the 60 Hz filtered components of transient measurements at the line terminals.**

The performance of the algorithms are evaluated through a parametric analysis of the variables present in the phenomenon. To accomplish this task, the modeling of a transmission line using data of one or more line terminals was taken into account.

Keywords: fault locator, transmission line, protection.

I. INTRODUCTION

In a transmission system, it is important to know the location of short-circuits, being this aspect studied through the digital fault locators systems.

In high voltage transmission lines, most of the faults (short-circuits) are transient. Eventually, these faults may become permanent as a result of burnt and damaged insulators, pollution, fall of towers or broken conductors.

Even in the case of non permanent faults, the identification of both type and fault-distance, are important, providing useful information in protection studies [1] and lightning performance behavior of the line.

This work presents a comparative analysis of some existent methods, which use data of one or more terminals of the line. For this purpose, two and three-terminal lines were regarded. A relatively wide parametric study of processed cases allows to evaluate the accuracy conditions of the methods considered.

The fault location methods described in this work [2,3,4,5] represent the main methods revised in the literature, and they use the steady state voltage and current phasors in each phase of one or more line terminals, besides some other line parameters are used.

II. FAULT LOCATION METHODS

A. Fault Location Using Data of Both Two Line Terminals

1) Two-Port Line Modeling Method

The following method [2] makes the equationing of the voltages in the faulted point considering the line as a two-port representation; it uses data of both terminals.

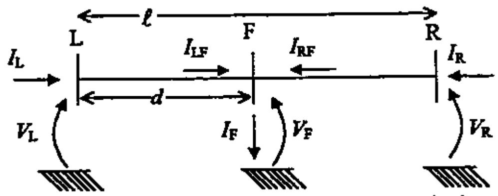

Fig. 1. Representation of a faulted transmission line

If data of the local terminal are used, then it can be written:

$$V_F = \cosh(\gamma d)V_L - Z_c \operatorname{senh}(\gamma d) I_L \qquad (1)$$

With the data of the remote terminal:

$$V_F = \cosh(\gamma(\ell - d))V_R - Z_c \operatorname{senh}(\gamma(\ell - d)) I_R \qquad (2)$$

Equating and simplifying (1) and (2), an expression that enables to calculate the fault-distance d, can be obtained:

$$d = \operatorname{atanh}\left(\frac{V_L - V_R\cosh(\gamma\ell) + Z_c I_R \sinh(\gamma\ell)}{Z_c I_L - V_R \sinh(\gamma\ell) + Z_c I_R \cosh(\gamma\ell)}\right)\frac{1}{\gamma} \qquad (3)$$

In equations (1) and (3), the values V_L, V_R, I_L, I_R, are the time synchronized phasors of the fundamental components of positive sequence; Z_c and γ are the respective surge impedance and propagation constant of the line, also for positive sequence.

2) Proposed data synchronization algorithm

The use of non synchronized data is done by introducing a new variable. Such a variable δ, represents the phase delay between local and remote terminal measurements.

$$V_R = V_R^{meas} e^{j\delta}$$
$$I_R = I_R^{meas} e^{j\delta} \qquad (4)$$

The angle δ is calculated solving by any numerical method as Newton-Raphson:

$$\operatorname{Im}\left[\operatorname{atanh}\left(\frac{V_L - V_R e^{j\delta}\cosh(\gamma\ell) + Z_c I_R e^{j\delta}\sinh(\gamma\ell)}{Z_c I_L - V_R e^{j\delta}\sinh(\gamma\ell) + Z_c I_R e^{j\delta}\cosh(\gamma\ell)}\right)\frac{1}{\gamma}\right] = 0 \qquad (5)$$

This angle can also be calculated using pre-fault values (obtained few cycles before the fault detection):

$$\delta = -\mathrm{j}\cdot\ln\left(\frac{\cosh(\gamma\ell)V_R^{pf} - Z_c \sinh(\gamma\ell) I_R^{pf}}{\cosh(\gamma\ell)V_L^{pf} - Z_c \sinh(\gamma\ell) I_L^{pf}}\right) \qquad (6)$$

3) Method Using the Line Series Impedance Matrix

Another fault location method [3] is based on the equationing of the voltages and currents under fault conditions.

It uses the series impedance matrix of the transmission line and considers the data of both line terminals.

Several publications present the same methodology, so this work could be considered representative of a family of methods.

The basic equations of this method provide the tree-phase voltage in the fault point, using the data of the two terminals of the transmission line.

$$[V_F]=[V_L]-d[Z_{a,b,c}][I_L] \quad (7)$$

$$[V_F]=[V_R]-(\ell-d)[Z_{a,b,c}][I_R] \quad (8)$$

Equating (7) and (8) and rearranging them, it is obtained:

$$[V_L]-[V_R]+\ell[Z_{a,b,c}][I_R]=d[Z_{a,b,c}]([I_L]+[I_R]) \quad (9)$$

From (9), estimation of the fault-distance can be found by using the least squares method in the following way:

$$d=(\overline{F}^{T}F)^{-1}\overline{F}^{T}L \quad (10)$$

Where:

$$L=[V_L]-[V_R]+[Z_{a,b,c}][I_R]\ell \quad (11)$$

$$F=[Z_{a,b,c}]([I_L]+[I_R]) \quad (12)$$

In expressions (7) to (12),

$\overline{F}^{T}$: is the transposed of the matrix F with the elements conjugated

$[Z_{a,b,c}]$: series impedance matrix of the line

$[V_L]$,$[V_R]$,$[I_L]$,$[I_R]$: three-phase vectors of voltage and current

B. Fault Location Using One Terminal Data

The fault location methods using only data of the local terminal of the line, uses some hypotheses to get an equationing of the fault-distance, disregarding the data of the remote terminal. Besides, some methods use the data of the network's pre-fault condition to minimize the error caused while considering some hypotheses.

The present method was proposed by Takagi [4], the nomenclature of Fig. 2 being adopted in this work, as follows:

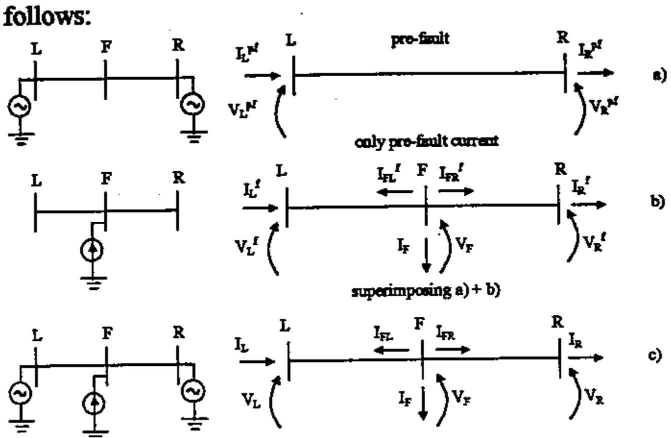

Fig. 2. Fault representation with super-imposed component

From Fig. 2 b), it can be verified that:

$$V_F=R_F I_F \quad (13)$$

$$I_F=-\; I_{FL}^{f}+I_{FR}^{f} \quad (14)$$

Defining:

$$K(d)=\frac{I_{FR}^{f}}{I_{FL}^{f}} \quad (15)$$

The use of (15) into (14), yields:

$$I_F=-K(d)I_{FL}^{f}-I_{FL}^{f} \quad (16)$$

Equation (16) applied into (13), gives:

$$V_F=-R_F I_{FL}^{f}\; 1+K(d) \quad (17)$$

As the values V_F and I_{LF}^{f} are not known, they can be determined using the data of the local terminal, through the two-port representation:

$$V_F=A(d)V_L-B(d)I_L \quad (18)$$

$$I_{FL}^{f}=C(d)V_L^{f}-D(d)I_L^{f} \quad (19)$$

$$A(d)=\cosh(\gamma d) \qquad B(d)=Z_c\,\mathrm{senh}(\gamma d)$$

$$C(d)=Z_c^{-1}\,\mathrm{senh}(\gamma d) \quad D(d)=A(d)$$

Using (18) and (19) into (17), gives:

$$A(d)V_L-B(d)I_L=-R_F\; C(d)V_L^{f}-D(d)I_L^{f}\; 1+K(d) \quad (20)$$

Which can be written as:

$$\frac{A(d)V_L-B(d)I_L}{C(d)V_L^{f}-D(d)I_L^{f}}=-R_F\; 1+K(d) \quad (21)$$

As for equation (21), the following hypotheses are considered:

- R_F (fault resistance) is purely resistive.
- $K\; d$ is a real number

The two previous hypotheses being considered, equation (21) would only have a real part; therefore, the following equation can be valid:

$$\mathrm{Im}\left(\frac{A(d)V_L-B(d)I_L}{C(d)V_L^{f}-D(d)I_L^{f}}\right)=0 \quad (22)$$

Equation (22) is applied to the case of a three-phase fault; it can be solved to obtain d; to accomplish this, some iterative methods are used (e.g. Newton-Raphson).

As for phase-to-ground faults, the expression to calculate the fault-distance uses data of the sequences 0 - 1 and 2:

$$\mathrm{Im}\left(\frac{V_F^0+V_F^1+V_F^2}{C^1(d)V_L^{1f}-D^1(d)I_L^{1f}}\right)=0 \quad (23)$$

$$V_F^0+V_F^1+V_F^2=3R_F I_F^1 \quad (24)$$

Whereas for a double-phase fault, it is used:

$$\mathrm{Im}\left(\frac{V_F^1-V_F^2}{C^1(d)V_L^{1f}-D^1(d)I_L^{1f}}\right)=0 \quad (25)$$

$$V_F^1-V_F^2=R_F I_F^1 \quad (26)$$

Finally, a double-phase-to-ground fault results in:

$$\mathrm{Im}\left(\frac{V_F^1-V_F^0}{C^0(d)V_L^{0f}-D^0(d)I_L^{0f}}\right)=0 \quad (27)$$

$$V_F^1-V_F^0=-3R_F I_F^0 \quad (28)$$

In equations (22) to (28), which derives the sequential diagrams for phase-to-ground, double-phase and double-phase-to-ground faults, the variables use the superindexes 0-1 and 2 to describe the sequential values of the variables used in Fig. 2.

In this method, it is important to store the pre-fault values of the voltages and currents appropriately. It is also useful to know the type of fault occurred, since the equationing for each case is different.

C. Fault Location Method for Three-Terminal Line Using Two-Port Representation

This method [5] is similar to that of the case of the two-terminal line [2], where data of the three terminals of the line were used. The fault-distance is given by the following expression:

$$d = \operatorname{atanh}\left(\frac{V_P - V_T\cosh(\gamma L_P) + Z_c I_{TP}\sinh(\gamma L_P)}{Z_c I_P - V_T\sinh(\gamma L_P) + Z_c I_{TP}\cosh(\gamma L_P)}\right)\frac{1}{\gamma} \quad (29)$$

Where:

$$I_{TP} = -C(L_Q)V_Q + A(L_Q)I_Q - C(L_R)V_R + A(L_R)I_R \quad (30)$$

$$V_T = A(L_R)V_R - B(L_R)I_R \quad (31)$$

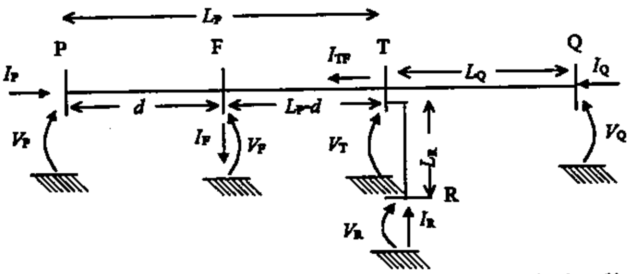

Fig. 3. Representation of a three-terminal transmission line with fault in section P-T

Equation (29) gives the fault-distance when a fault occurs in section P-T. In case the fault occurs in a different section, the equationing will be similar, except that the variables will correspond to the respective section.

One way to identify the section in which the fault has occurred is to calculate the voltage V_T as a function of the voltage and current in each of the three terminals of the transmission line, being the sections without fault those in which the calculated voltage V_T, are equal to one another:

$$\begin{aligned} V_T &= A(L_P)V_P - B(L_P)I_P \\ V_T &= A(L_Q)V_Q - B(L_Q)I_Q \\ V_T &= A(L_R)V_R - B(L_R)I_R \end{aligned} \quad (32)$$

1) Proposed Data Synchronization Algorithm

Considering that the fault occurred in section P-T, and the terminal P as reference to the phase angles, its has:

$$V_Q = V_Q^{meas} e^{j\varepsilon} \qquad I_Q^1 = I_Q^{meas} e^{j\varepsilon} \quad (33)$$

$$V_R^1 = V_R^{meas} e^{j\delta} \qquad I_R = I_R^{meas} e^{j\delta} \quad (34)$$

The phase mismatch between data of terminals P,Q and R also can be obtained considering the voltage in terminal T calculated using two-port representation and pre-fault values.

Adopting P as reference terminal, comparing the V_T values obtained using data of terminals P,Q and P,R it is possible to directly calculate the phase mismatch data of line terminals, using the expressions:

$$\varepsilon = -j\cdot\ln\left(\frac{\cosh(\gamma L_Q)V_Q^{pf} - Z_c\,\mathrm{senh}(\gamma L_Q)I_Q^{pf}}{\cosh(\gamma L_P)V_P^{pf} - Z_c\,\mathrm{senh}(\gamma L_P)I_P^{pf}}\right) \quad (35)$$

$$\delta = -j\cdot\ln\left(\frac{\cosh(\gamma L_R)V_R^{pf} - Z_c\,\mathrm{senh}(\gamma L_R)I_R^{pf}}{\cosh(\gamma L_P)V_P^{pf} - Z_c\,\mathrm{senh}(\gamma L_P)I_P^{pf}}\right) \quad (36)$$

III. DIGITAL FILTERING USING THE LEAST SQUARES METHOD

An example of the digital filtering method is presented in [6]. In this work, the digital filtering was implemented using the least squares method, considering the following fitting function for the voltage and current waveforms:

$$\begin{aligned} &f(t) = a_1\cos(\omega t) + a_2\,\mathrm{sen}(\omega t) + a_3\cos(2\omega t) + \ldots \\ &a_4\,\mathrm{sen}(2\omega t) + a_{N-3}\cos((N/2-1)\omega t) + \ldots \\ &a_{N-2}\,\mathrm{sen}((N/2-1)\omega t) + a_{N-1} + a_N t \end{aligned} \quad (37)$$

It is intended, by means of equation (37), to approach the waveforms for the harmonic components and for an exponential component (whose original function was simplified to a straight line) so that this exponential part would not affect the calculation of the fundamental component.

The frequency response for the filters sine and cosine calculated using expression (37) in series with a digital Butterworth low-pass filter [7], presents unitary gain for the fundamental frequency and null gain for the other harmonics.

The algorithm of the digital filtering was tested based in the waveforms of voltage and current in the line terminals, simulating a three-phase fault in the network depicted in Fig. 4.

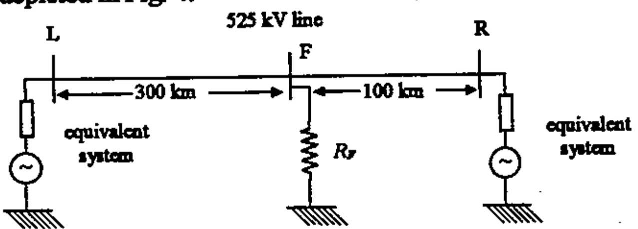

Fig. 4. Network for testing the digital filtering algorithm.

The typical current waveform and the output of the digital filter are shown below:

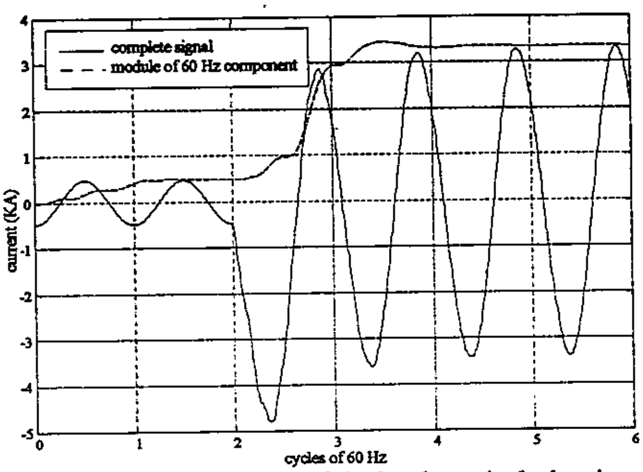

Fig. 5. Current in phase C of the local terminal, showing transient components and magnitude of the fundamental

IV. TEST OF FAULT LOCATION METHODS

The tests aim is to evaluate the effect in the algorithms accuracy caused by variations of the following factors: fault-distance, fault resistance, fault type, line length and parameters of the equivalent network. The variation effect of the fault instant was not analyzed, this being a test frequently used in the literature to evaluate the behavior of the digital filtering for different levels of the exponential component.

For a two-terminal line network as the one depicted in Fig 4, lengths comprising 50 km and 400 km were used. Simulations were evaluated by using ATP program [8]; the line was modeled regarding some conditions such as: having distributed parameters and being continually transposed.

The line length affects greatly when considering the line-to-ground capacitance, mainly when the line is long; thus, affecting the hypotheses assumed in this paper, justifiyng an analysis of the effect of the line length.

For a three-terminal line, the following network was used.

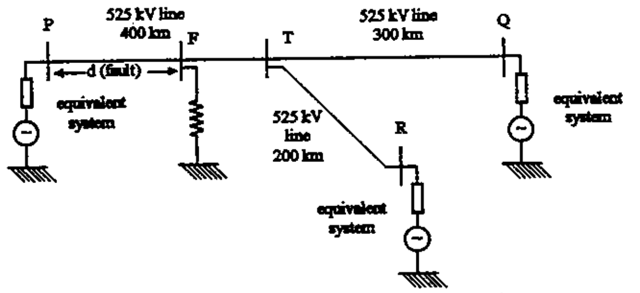

Fig. 6. Three terminal line network

A. Results of the Tests for a Two-Terminal Line

Figure 7 shows the fault distance along the time for a phase-to-ground fault at 300 km from the local terminal of the 400 km line. For result analysis purposes, the distance values obtained in the end of the sixth cycle in the simulation, were considered (last available instant).

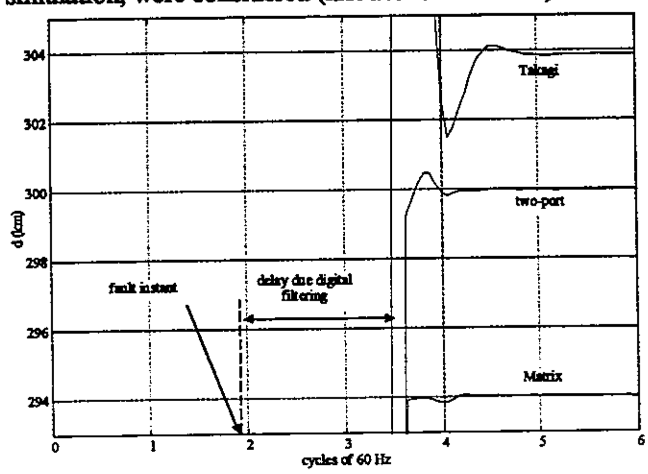

Fig. 7. Fault-distance to the local terminal

1) Effect of the Fault-Distance Variation

As for the analysis of the fault-distance variation effect, while observing the performance of the studied algorithms, cases of phase-to-ground and three-phase faults, were simulated. In this case long lines were regarded, having a fault resistance of 10 Ω.

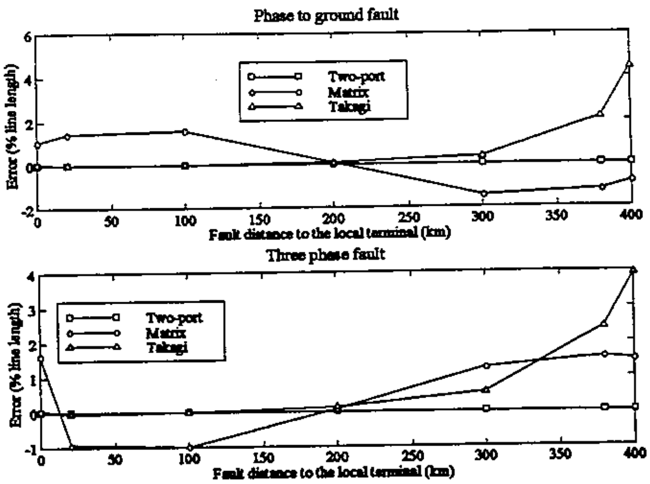

Fig. 8. Effect of the fault-distance

It can be verified that the two-port method is insensitive to the variation of the fault-distance. The matrix method is accurate for faults in the middle of the line, whereas the Takagi method is more inaccurate as the fault-distance from the local terminal increases.

2) Effect of the Fault Resistance Variation

There were simulated cases of faults such as a 35 km fault-distance (short line) and a 300 km fault-distance (long line) with fault resistance varying in a range of 0 to 40 Ω.

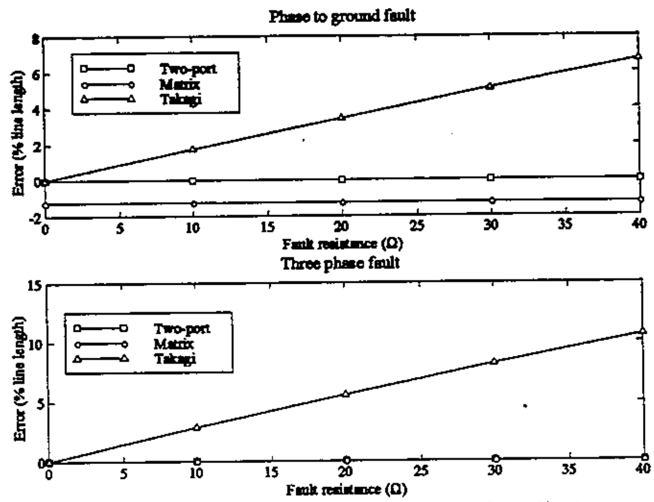

Fig. 9. Effect of the fault resistance (short line)

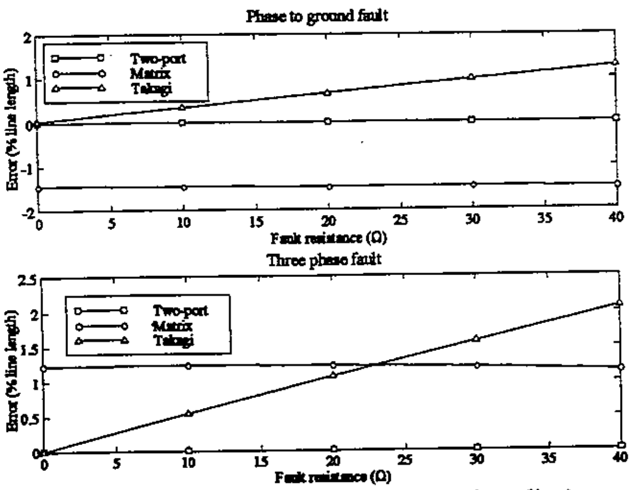

Fig. 10. Effect of the fault resistance (long line)

As can be observed in the figures above, the two-port method has its accuracy independent of the fault resistance, the same occurring with the matrix method. On the other hand, the Takagi method is more inaccurate as the fault resistance increases.

3) Effect of the Fault Type Variation

All the possible types of faults were also simulated, with fault distances of 35 km for short lines and 300 km for long lines, being the fault resistance 10 Ω.

It was observed that the two-port method does not present variations in the accuracy when changing the fault type. For short lines, the matrix method is accurate only for those faults that do not involve the ground. In relation to the Takagi method, its inaccuracy has been verified in those cases involving a three-phase fault.

4) Variation Effect of the Equivalent Impedance Magnitude in the Local Terminal

There were also simulated cases of faults with fault-distance of 35 km for short line. The values of the magnitude of the equivalent impedance in the local terminal used were 20%, 50% 100% and 200% of the base case, in which the local terminal short circuit power values, are: $S_{sc}3\phi$ =13,8 GVA and $S_{sc}\phi g$ =14,82 GVA.

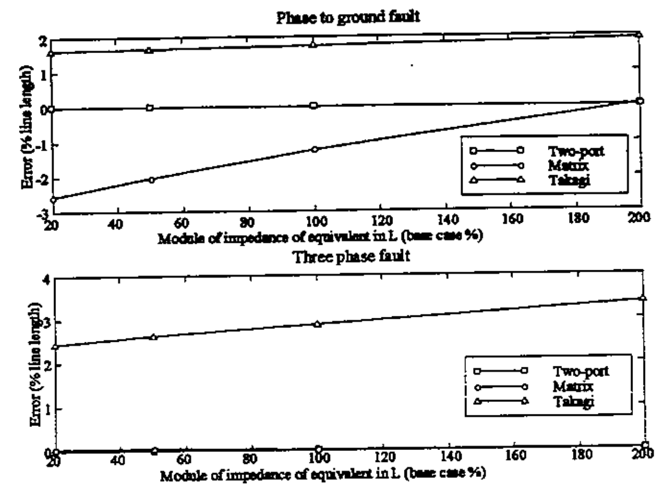

Fig. 11. Effect of the equivalent impedance magnitude

Figure 11 shows that the accuracy of the methods has dependency with the equivalent impedance magnitude except for the two-port method.

5) Variation Effect of the Equivalent Impedance Phase Angle in the Local Terminal

Fault cases with fault distances of 35 km in a short line were simulated. Different values for the equivalent impedance phase angle in the local terminal, have been used; the value of the impedance magnitude was kept invariable, which corresponded to varying the resistive component.

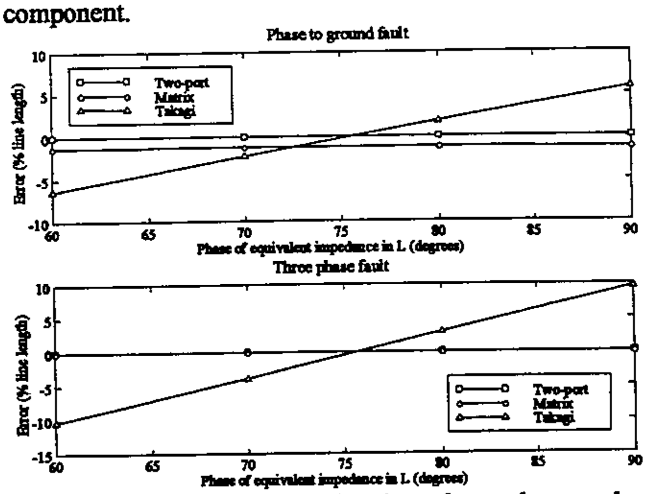

Fig. 12. Effect of the equivalent impedance phase angle (short line)

For the case of long lines, the results were practically the same as those for the short line. It can be verified that only the Takagi method's accuracy was been affected by the value of the equivalent impedance phase angle.

6) Test of Data Synchronization Algorithm

The data synchronization algorithm for the two-port method, was also tested; to achieve this, a phase-to-ground fault located at 300 km from the local terminal with a fault resistance of 10 Ω, was simulated.

Table I – Delaying effect, between local and remote terminal data

delay (degrees)	fault-distance (km)	absolute error (km)	relative error (%)
0	299.97	-0.03	-0.01
-45	299.97	-0.03	-0.01
-90	299.96	-0.04	-0.01
-135	299.97	-0.03	-0.01
-180	299.99	-0.01	0.00
-225	299.99	-0.01	0.00
-270	300.02	0.02	0.00
-315	300.00	0.00	0.00

B. Results for Three-Terminal Line Fault Locator Method

The tests have shown that the accuracy of the algorithm is not affected by variations like the fault-distance, fault resistance or the type of fault. Results of fault-distance variations regarding a ground-to-phase and three phase faults in section P-T with a fault resistance of 10 Ω.

Table II - Fault-distance variation effect

	fault-distance (km)	calculated fault-distance (km)	absolute error (km)	relative error (%)
Phase-to-ground faults	0	-0,03	-0,03	-0,01
	100	99,87	-0,13	-0,03
	200	200,05	0,05	0,01
	300	300,01	0,01	0,00
	400	399,97	-0,03	-0,01
three-phase fault	0	-0,08	-0,08	-0,02
	100	99,97	-0,03	-0,01
	200	200,02	0,02	0,00
	300	300,00	0,00	0,00
	400	400,00	0,00	0,00

From table II, the accuracy of the method can be verified, in which a maximum fault-distance error of 80 m was obtained.

1) Test of Data Synchronization Algorithm

The data synchronization algorithm was also tested; to achieve this, a phase-to-ground fault located at 300 km from terminal P, in section P-T, with a fault resistance of 10 Ω, was simulated.

Table III – Phase delay effect

Q-P delay (degrees)	R-P delay (degrees)	fault distance (km)	absolute error (km)	relative error (%)
45	45	299.93	-0.07	-0.02
90	45	299.78	-0.22	-0.05
180	45	299.98	-0.02	-0.01
270	45	299.92	-0.08	-0.02
45	90	299.90	-0.10	-0.02
90	90	299.76	-0.24	-0.06
180	90	299.96	-0.04	-0.01
270	90	299.90	-0.10	-0.03

V. CONCLUSIONS

In this work, an analysis that involved a considerable number of evaluations of the behavior of some well-known algorithms, due to alterations of some influential variables during the short circuit, was performed.

These evaluations allowed to perform a comparative analysis of the algorithms studied due to the several conditions of electric networks. To make obtaining these results possible, which is presented in a condensed form in this work, the fault locations algorithms and the methods of digital filtering were implemented using data of ATP simulations, making possible the obtaining of parametric results. The language MODELS of ATP was used in the simulations to perform analog filtering (anti-aliasing) [7], and sampling of voltages and currents in the line terminals.

The results showed that the more accurate fault location methods are those obtained starting from the equationing of the voltages and currents in all the line terminals, with the two-port representation and that model the lines considering distributed parameters, for two terminal lines [2], and three terminal lines [3], being their accuracy independent of the several analyzed factors, such as fault-distance and fault resistance.

The proposed synchronization algorithm for the two-port methods [2,3], for two and three terminal lines, showed that it is possible to use unsynchronized data of two and three terminals without losing accuracy, making the off-line use of these fault location methods possible.

The method proposed in [4], has the accuracy decreased in the case of faults distant of the local terminal, high fault resistance, and equivalent with big resistive part; even so its largest advantage is to use data of just one line terminal.

The method with use of three-phase matrix [3] presented larger imprecision for the case of long lines, due to the fact of considering neither hyperbolic corrections nor the line capacitance.

VI. REFERENCES

[1] A.G. Phadke, J.S. Thorp, *Computer Relaying for Power Systems*, Research Studies Press, Tauton, 1988.

[2] A.T. Johns, S. Jamali, "Accurate Fault Location Technique for Power Transmission Lines", *IEE Proceedings Generation, Transmission and Distribution*, vol. 137, n. 6, 1990, pp. 395-402.

[3] A.A Girgis, D.G. Hart, W.L. Peterson, "A New Fault Location Technique for Two and Three-Terminal Lines", *IEEE Transactions on Power Delivery*, vol. 7, n. 1, 1992, pp. 98-107.

[4] T. Takagi et al., "Development of a New Type Fault Locator Using the One-Terminal Voltage and Current Data", *IEEE Transactions on Power Apparatus and Systems*, vol. 101, n. 8, 1981, pp. 2892-2898.

[5] R.K. Aggarwal et al., "A Practical Approach to Accurate Fault Location on Extra High Voltage Teed Feeders", *IEEE Transactions on Power Delivery*, vol. 8, n. 3, 1993, pp. 874-83.

[6] M. S. Sachdev, M.A Nagpal, "Recursive Least Squares Algorithm for Power System Relaying and Measurement Applications", *IEEE Transactions on Power Delivery*, vol. 6, n. 3, 1991, pp. 1008-1015.

[7] A.V. Oppenheim, R.W. Schafer, *Digital Signal Processing*, Englewood Cliffs, Prentice-Hall, New Jersey, 1975.

[8] Leuven EMTP Center, *ATP: Alternative Transients Program Rule Book*. Leuven, U.K., 1987.